Organic–Inorganic Character of Plasma-Polymerized Hexamethyldisiloxane

L. ZURI, M. S. SILVERSTEIN,* and M. NARKIS

Departments of Chemical and Materials Engineering, Technion–Israel Institute of Technology, Haifa 32000, Israel

SYNOPSIS

Plasma polymerization is a useful method for depositing thin films on substrates. The films formed are cross-linked, and their character depends on the plasma polymerization process conditions. The influence of power and monomer flow rate on the character of plasma-polymerized hexamethyldisiloxane (PPHMDSO) was investigated. The deposition rate increased strongly with HMDSO flow rate at low powers, indicating that the plasma is monomer-deficient. Increasing the power yielded a rapid drop in deposition rate, which reached a relatively flow rate-independent plateau at high powers. At high flow rates and low powers, the similarity between the plasma polymer with its high hydrocarbon concentration and the monomer was greatest. At high powers, the monomer was more intensively fragmented yielding a more inorganic structure rich in silicon and oxygen. Generally, the plasma polymer seems to be a silicon-oxygen network with short hydrocarbon chains that may include hydroxyl and/or carbonyl groups attached to the silicon in the backbone. The inorganic nature of the plasma polymer at high powers and low flow rates is reflected in its relatively high polar component of surface tension. © 1996 John Wiley & Sons, Inc.

INTRODUCTION

Plasma polymerization is a unique process for the formation of ultrathin films. Any organic compound that can be vaporized is a monomer that can be plasma-polymerized. A variety of new polymer thin films can be created through plasma polymerization. The polymer formed cannot be described in terms of repeating units, owing to the growth mechanism based on the random assembly of various monomer fragments.[1] The chemical structure of plasma polymers strongly depends on the fragmentation of the monomer.[1] This fragmentation depends not only on the chemical composition and structure of the monomer[2–4] but also on the polymer deposition process conditions in the glow discharge, such as pressure, power, flow rate, current densities, temperature, etc. By varying these process parameters, materials with different chemical compositions and structures can be obtained from the same monomer.[5–8]

* To whom correspondence should be addressed.

Journal of Applied Polymer Science, Vol. 62, 2147–2154 (1996)
© 1996 John Wiley & Sons, Inc. CCC 0021-8995/96/122147-08

Plasma polymers produced from a variety of organosilicon monomers have been studied due to the general interest in conventional organosilicon polymers and interest in organosilicon polymer films for silicon-based microelectronic applications. Organosilicon monomers are volatile, easy to use, nontoxic, relatively inexpensive, and available from commercial sources. The chemical structure of organosilicon plasma polymers can be tailored for applications such as insulators, composite thin films,[9] wave guides,[10,11] and separation membranes.[12–14] Separation processes require a high permeate flux, and the flux of the permeate is inversely proportional to the membrane thickness. A composite membrane structure composed of a thin dense permselective layer and a porous supporting substrate is therefore preferable.

Plasma polymerization is useful technique for the formation of the described composite membranes. A pinhole-free ultrathin layer can be deposited on a porous substrate, yielding a composite polymer membrane that can surpass the properties of membranes formed by conventional processes. Furthermore, plasma polymers are crosslinked and, thus, are more thermally stable and much less soluble in

organic solvents. The present article focuses on the relationships between the plasma polymerization conditions and the chemical structure of thin films of plasma-polymerized hexamethyldisiloxane (PPHMDSO).

EXPERIMENTAL

Materials

Hexamethyldisiloxane (HMDSO, Aldrich) was used as a monomer without further purification. The plasma polymers were deposited on rectangular glass slides. KBr was used for spectroscopic analysis (Merck) after drying. α-bromonaphthalene (Kodak) was used for contact angle measurements.

Plasma Reactor and Polymerization Procedure

A March Jupiter III parallel plate 13.56 MHz radio frequency plasma reactor was the basis of the plasma reactor system. The configuration of the process system is shown in Figure 1. The chamber consists of 21 cm diameter anodized aluminum parallel plate electrodes separated by 3.8 cm. The electrodes are water-cooled to control the substrate temperature during processing. The plasma power can be varied between 10–250 W. The experimental procedure is as follows. The system was evacuated to 0.18 torr (1 torr = 133.3 Pa) via a liquid nitrogen cold trap. Argon was introduced directly into the reactor chamber at 1 torr, for 3–5 min, and the system was evacuated again to 0.18 torr. Argon, now being used as a carrier gas, was passed through a flask containing the monomer and into the reactor. The individual flow rates of HMDSO and carrier gas were determined by the measurement of the rates of pressure increase when the pumping was abruptly stopped during steady-state flow.[1] The flow rate of the monomer was on the order of 14.4–29 cm^3 (STP) per minute (sccm) was determined by the monomer flow rate (before the plasma was ignited). The initial reactor pressure was determined by the monomer flow rate. After the flow rate and initial pressure were stabilized, the plasma was ignited. The operating conditions for several polymerization experiments of interest are shown in Table I. At the end of the polymerization, the monomer inlet was closed, and the system was evacuated to 0.18 torr and maintained at that pressure for 10 min. The reactor was opened to the atmosphere, and the samples were removed and stored in a dessicator.

Characterization

Electron Spectroscopy for Chemical Analysis

The chemical composition of the surfaces of plasma films deposited on glass slides was studied using electron spectroscopy for chemical analysis (ESCA). A photoelectron spectrometer (Perkin Elmer Physical Electronics 555 ESCA/Auger) with an Al K_α source was used. The atomic concentrations were determined with an accuracy of 1% in a low resolution scan and the nature of the bonds with carbon

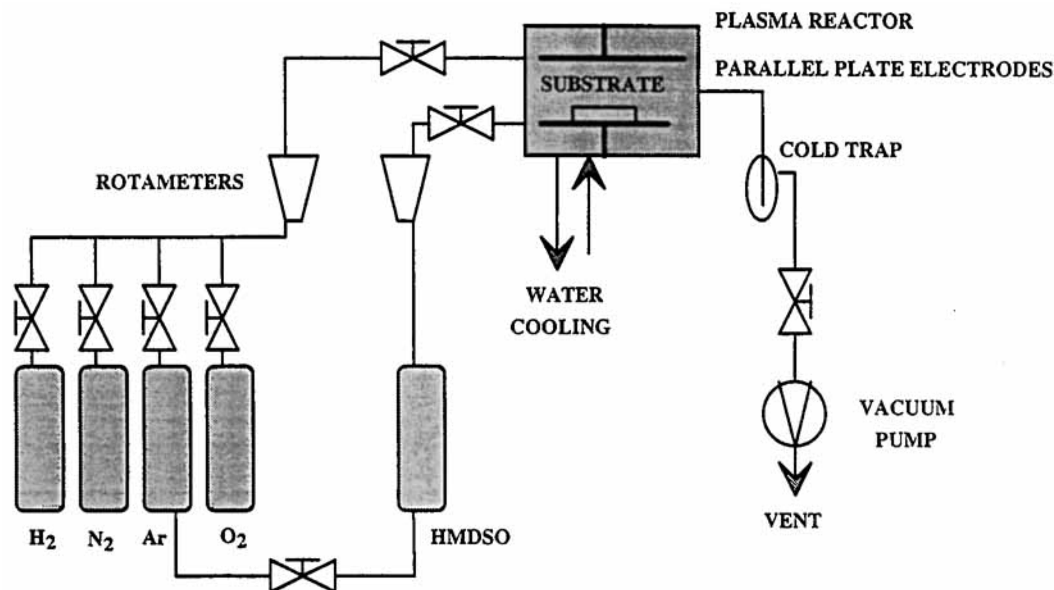

Figure 1

Table I Operating Conditions for Plasma Polymerization Experiments

Exp. #	Flow Rate (sccm)	Power (W)	Initial Pressure (torr)
10-50	10	50	0.6
10-250	10	250	0.6
25-50	25	50	1.1
25-250	25	250	1.1

and silicon in high resolution C_{1s} and Si_{2p} scan, respectively. The C_{1s} and Si_{2p} spectra were deconvoluted using a curve-fitting program.[15] Prior to deconvolution, the background was subtracted from the spectrum using one iteration of the Shirley method.[15] The curve-fitting variables for C_{1s} peak were the peak heights and the full width at half maximum (FWHM). A combination of Gaussian and Lorentzian distributions was assumed,[15] and the same peak positions were used for all the plasma polymers. For Si_{2p}, the curve-fitting variables were the positions of the peaks (four to five peaks) and their heights. A Gaussian distribution was assumed, and the FWHM was determined to be 1.1. ESCA was also used to investigate the composition beneath the surface after removing 100 Å by sputtering with argon.

Fourier Transform Infrared Spectroscopy

Transmission Fourier transform infrared spectroscopy (FT IR) was performed on KBr pellets placed in the plasma reactor. The plasma films were deposited using these pellets as substrates. The plasma films were analyzed using a Nicollet Impact 400 infrared Fourier transform spectrometer.

Surface Tension

The contact angles (θ) between either distilled water or α-bromonaphthalene and the plasma polymer films deposited on glass slides were measured at room temperature using a Kernco goniometer, with an advancing droplet technique.[16] The contact angle data were analyzed to determine the dispersive and polar components of the total surface tension (γ^d, γ^p, and γ respectively).[17] The relationship between the components of the surface tension and contact angle is expressed by:

$$(1 + \cos\theta) = \frac{2}{\gamma_l}\left[(\gamma_s^d \cdot \gamma_l^d)^{1/2} + (\gamma_s^p \cdot \gamma_l^p)^{1/2}\right] \quad (1)$$

where s represents solid and l represents liquid. Equation (1) has two unknowns, γ_s^d and γ_s^p, but is simplified in eq. (2) for α-bromonaphthalene, which has no polar surface tension component:

$$\gamma_s^d = \frac{[\gamma_l(1 + \cos\theta)]^2}{4\gamma_l^d} \quad (2)$$

once γ_s^d is determined from eq. (2) using α-bromonaphthalene ($\gamma_s^d = 44.6$ mN/m; $\gamma_s^p = 0$ mN/m), when γ_s^p can be determined from eq. (1) and the contact angle with water ($\gamma_s^d = 21.8$ mN/m; $\gamma_s^p = 51$ mN/m).

RESULTS AND DISCUSSION

Deposition Rate

Plasma-polymerized HMDSO (PPHMDSO) films were transparent and yellow to brown, depending on the deposition conditions. The films were smooth and homogeneous.

The deposition rate was independent of deposition time, as expected from a steady state reactor process. All the films adhered strongly to the glass substrate. The deposition rate of PPHMDSO varied from 1.7–11 μg/(cm^2 min), depending on power and monomer flow rate, as shown in Figure 2. The highest deposition rate occurred at the lowest power and the highest flow rate, decreasing with increasing power and with decreasing flow rate. The deposition rate is most sensitive to flow rate at low powers and most sensitive to power at high flow rates. Yasuda[1] has labelled two regimes which describe plasma process behavior: a monomer-deficient region in which the deposition rate is proportional to flow rate is independent of the power, and an energy-deficient region in which the deposition rate is proportional

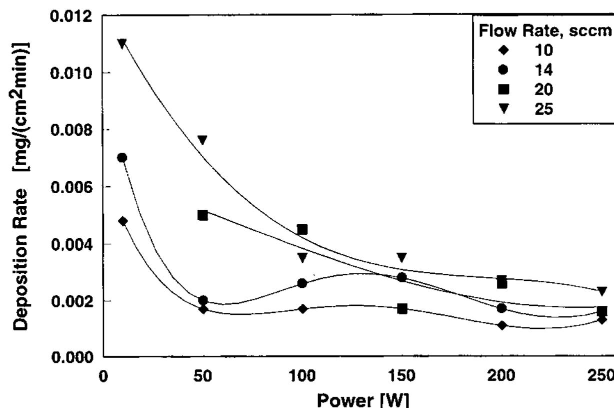

Figure 2

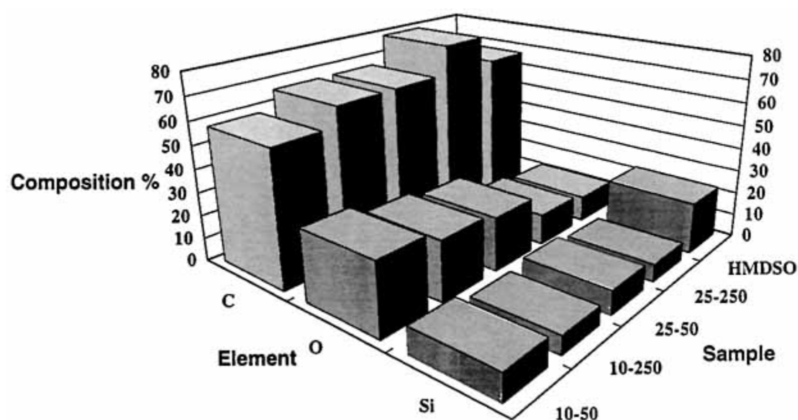

Figure 3

to the power but is independent of the flow rate. The results in Figure 2 are quite different from typical plasma polymerization. The strong increase in deposition rate with flow rate at low powers indicates that the polymerization is within the monomer-deficient region. Increasing the power in this region yields even more intensive monomer fragmentation. The rapid drop in deposition rate with increasing the power indicates that the excess power forms even smaller fragments which do not combine to form larger molecules in the reactor. Above 200 W, the system reaches an energy saturation, and the smallest fragments are formed. The effects of forming these smaller fragments are seen in the chemical structure.

Molecular Structure

The low resolution ESCA spectra for PPHMDSO exhibited peaks corresponding to C_{1s}, O_{1s}, Si_{2s}, and Si_{2p}. The elemental compositions from ESCA are shown in Figure 3, and the Si/O and Si/C ratios are shown in Figure 4. The different PPHMDSO films

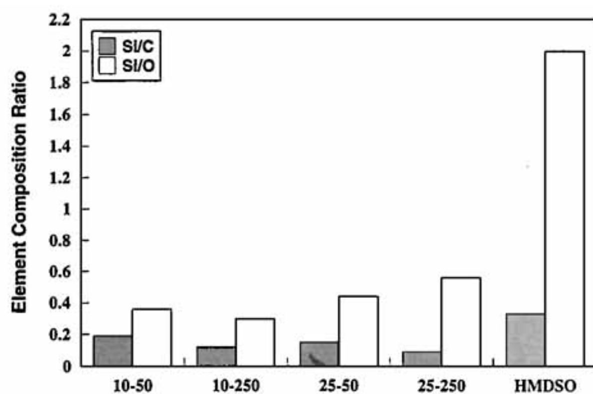

Figure 4

contain 13–31% oxygen, which is more than the approximately 11% in the monomer. The reaction of atmospheric oxygen with long-lived radicals is commonly found in plasma polymer films and can explain the abundance of oxygen.[18,19] ESCA spectra taken following argon ion sputtering that removed 100 Å from the surface seems to indicate that there is abundant oxygen (20–30%) throughout the PPHMDSO films and not only at the surface.

The silicon/carbon ratio in the plasma polymer (Fig. 4) is smaller than that of the monomer. At high flow rates and low powers, when the deposition rate is high, the plasma polymer mostly resembles the monomer. When the flow rate decreases, the Si/C ratio increases, indicating a more inorganic plasma polymer. At high powers, the monomer fragmentation is more intensive, yielding new chemical structures. When the flow rate decreases, the Si/C ratio increases, indicating a more inorganic plasma polymer.

The C_{1s} spectra were deconvoluted into C—C, C—O, C=O, and C—Si contributions with binding energies of 285, 286.5, 288, and 284.3 eV, respectively. The positions of the deconvoluted C_{1s} component peaks were similar to the reference peaks reported in the literature.[20,21] Figure 5 shows a typical C_{1s} peak deconvolution for the 25–50 sample. HMDSO, the monomer, does not contain C—O or C=O bonds. These groups are typically found in the plasma polymerization of siloxane compounds[6,20] and result from the reaction of atmospheric oxygen with long-lived radicals in the plasma polymer. The deconvolution of the Si_{2p} peak is much more complicated than for the C_{1s} peak. The deconvolution of various Si_{2p} peaks yielded Si—C peaks between 101 and 101.6 eV and Si—O peaks between 102.2 and 102.8 eV, both consistent with literature values.[20–23] In addition, there is a significant tail at higher binding energies in the Si_{2p} spectra that re-

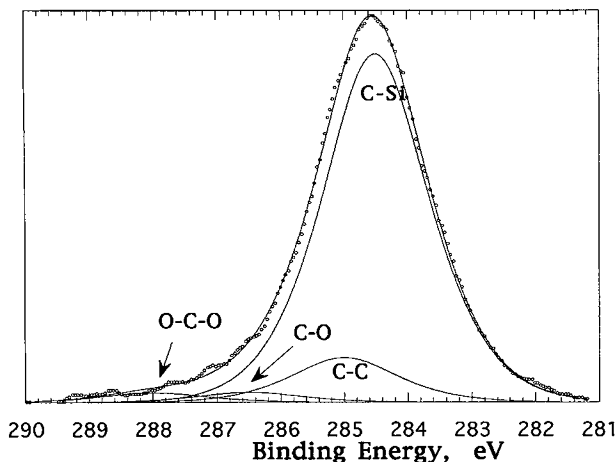

Figure 5

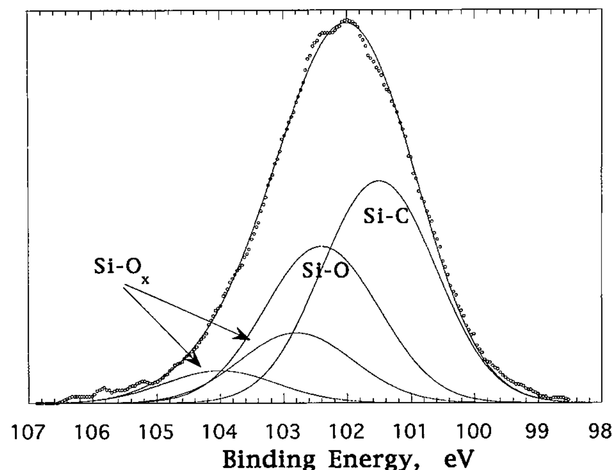

Figure 6

sults from various species of Si — O_x ($x > 1$). Figure 6 shows a typical Si_{2p} peak deconvolution for the 25-50 sample.

A graphical summary of the elemental analysis including C_{1s} and Si_{2p} peak deconvolutions is shown in Figure 7. All the samples have significant amounts of C — O bonds as a result of the reaction of atmospheric oxygen with the free radicals in the plasma polymer. From the ESCA results, it seems that the structure is more sensitive to flow rate than to power. Figure 7 shows that at high flow rates (at both high and low powers), the samples have high concentrations of C — Si bonds reflected in both the C_{1s} and Si_{2p} deconvolutions. On the other hand, at low flow rates (at both high and low powers), the Si — C bonds concentration decreases significantly. These observations indicates that at low flow rates, monomer fragmentation increases as the plasma polymerization is driven further into monomer-deficient conditions. Most of the carbon is bound to either silicon (as in the monomer) or to carbon. Silicon is bound to either carbon or oxygen (as in the monomer). These results suggest that the plasma polymer is actually a silicon-oxygen network with short hydrocarbon chains containing hydroxyl and carbonyl groups attached to the silicon in the backbone.

FT IR spectra of PPHMDSO at different polymerization conditions are shown in Figure 8. FT IR spectra of PPHMDSO at 50 W for both high and low monomer flow rates is shown, as well as FT IR spectra of PPHMDSO at 250 W for both high and low monomer flow rates. The FT IR spectral peak positions are listed in Table II.[24] The spectra shown in Figure 8 have many characteristic absorption bands in common: the methyl (CH_3) stretching vibration at 2940 and 2882 cm^{-1} (asymmetric and symmetric vibrations); the Si — CH_3 asymmetric and symmetric deformation at 1425 and 1263 cm^{-1}, respectively; the Si — $(CH_3)_3$ stretching vibration at 860 cm^{-1}; and the strong band from the Si — O stretching vibration at 1050 cm^{-1}. The peak at 2400 cm^{-1} resulted from traces of atmospheric CO_2 that remained in the spectrometer cell.

The ratios of the absorption peak heights for Si — O (1050 cm^{-1})/CH_3 (2940 cm^{-1}) and for Si — O (1050 cm^{-1})/Si — $(CH_3)_3$ (860 cm^{-1}) are shown in

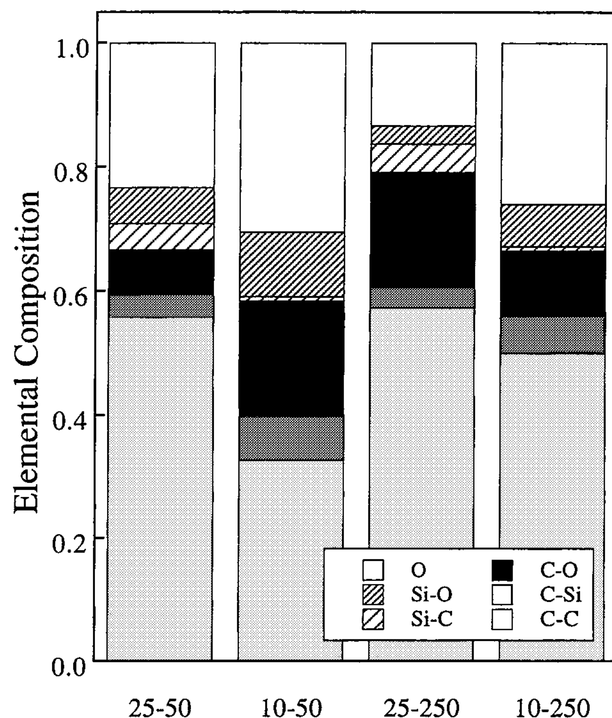

Figure 7

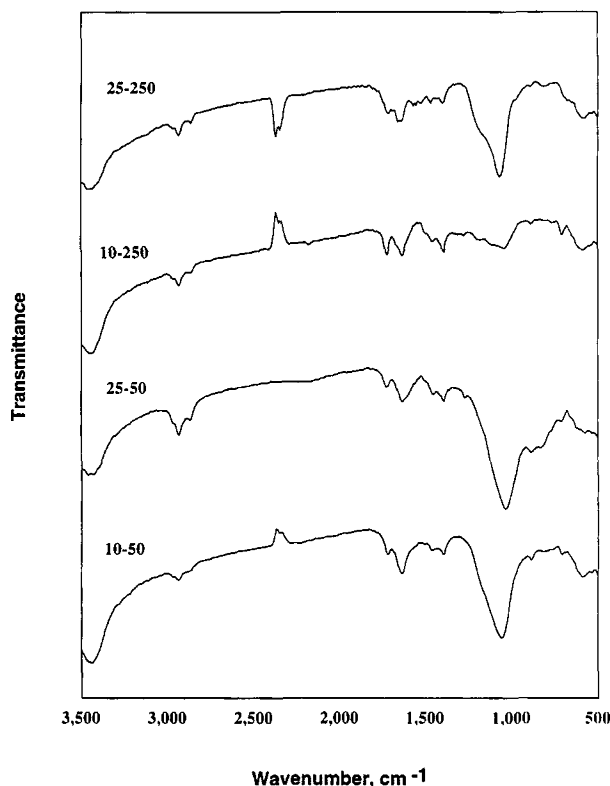

Figure 8

Figure 9 for different polymerization conditions. The Si—O bonds represent the inorganic nature of the films, while the CH_3 and the Si—$(CH_3)_3$ bond represent the organic nature. The ratios reflect the fundamental differences in the chemical structure associated with the balance between the organic and inorganic nature of the plasma polymer. The Si—O/CH_3 ratio and the Si—O/Si—$(CH_3)_3$ ratio decrease with increasing power at low monomer flow rate, while the opposite is true at high flow rates.

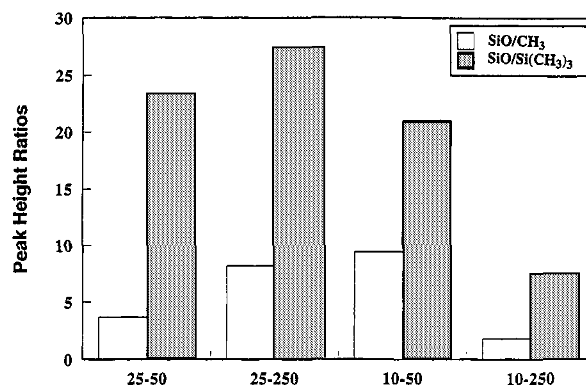

Figure 9

The intensive fragmentation of the monomer at high powers creates Si—H (2175 cm^{-1}) and C=O groups (1700 cm^{-1}). At low powers, changing the flow rate yields more significant effects. The Si—O/CH_3 ratio decreases with increasing flow rate since introducing more monomer to the relatively energy-poor plasma yields less fragmentation and the resulting polymer retains more of the original monomer structure. The relatively constant Si—O/Si—$(CH_3)_3$ ratio at low powers also reflects the low-energy plasma-generating polymers, which retain more of the original monomer structure. At low powers, there is no evidence of Si—H peaks, and the C=O peaks are less prominent, confirming that fragmentation is less intensive, complementing the ESCA analysis. The low Si—O concentration in Figure 9 for 10-250 is not understood, especially in light of other results.

Figure 10 shows proposed chemical structure models of PPHMDSO films at different conditions. The carbon is bound to silicon as short hydrocarbon chains that can include carbonyl or hydroxyl groups. At high powers, the silicon may also be attached to

Table II Infrared Frequencies and Band Assignments*

Frequency (cm^{-1})	Band Assignment
2972–2952	—CH_3 asymmetric stretching
2882–2862	—CH_3 symmetric stretching
2100–2150	Si—H stretching
1700	C=O stretching
1410–1440	Si—CH_3 asymmetric deformation
1255–1280	Si—CH_3 symmetric deformation
1000–1100	Si=O asymmetric stretching
760–860	Si—$(CH_3)_3$ symmetric deformation

* See Colthup et al.[24]

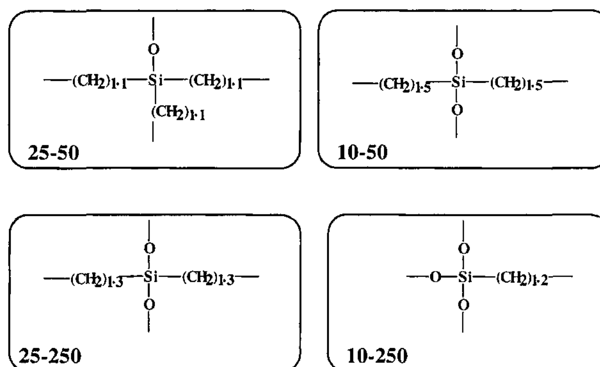

Figure 10

hydrogen as a result of intensive fragmentation. The amount of oxygen bound to silicon is a function of the polymerization conditions, and its variation indicates that the polymer changes from dominantly organic (25-50) to dominantly inorganic (10-250). The surface layers are expected to be richer in oxygen and include some hydroxyl groups.

Surface Tension

Figure 11 shows the total surface tension of the plasma polymer films divided into dispersive and polar components. The dispersive components of the films are rather similar, approximately 42 mN/m. The polar components vary from a minimum of 6 mN/m for (25-50) to a maximum of 22 mN/m for (10-250). The plasma polymer surface tension is very high compared to that of typical PDMSO surfaces, 20 mN/m.[25] As all the films are smooth, the changes in surface tension are directly related to the surface chemistry of the films. The relatively high polar surface tension reflects the high concentration of carbon-oxygen groups (e.g., hydroxyl) incorporated onto the surface by the reaction of free radicals with atmospheric oxygen. The increase in the polar contact angle with decreasing flow rate supports the different chemical structures described in Figure 10. The most monomer-starved plasma polymer (at high power and low flow rate) has a dominantly inorganic nature reflected in its large polar surface tension. The least monomer-starved plasma polymer (at low power and high flow rate) is more organic in nature and has the lowest polar surface tension.

The chemical structure of the plasma polymer can be controlled through the polymerization conditions. In this research, the influence of the flow rate and the power on the chemical structure was described. These conditions affect the fragmentation of the monomer introduced into the glow discharge. When the power is high and the amount of the monomer is low, the molecules are intensively fragmented. When the power is low and the flow rate is high, the decrease in energy per mass yields less intensive fragmentation and plasma polymers more closely resemble the chemical structure of the monomer. Studies on the relationships between the chemical structure of these films and their potential application as membranes for per vaporation separation processes are currently being undertaken.

CONCLUSIONS

In summary, the following conclusion can be drawn from the results presented here.

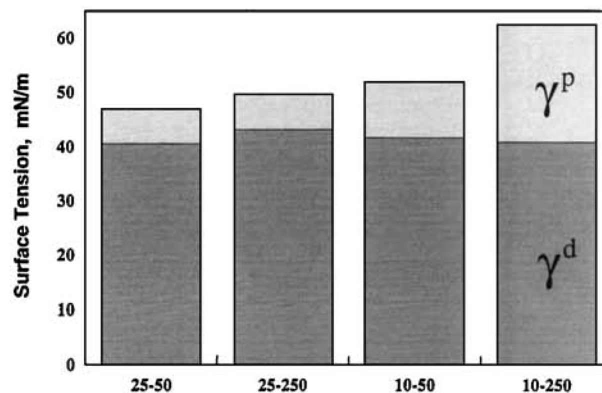

- Plasma polymerization of HMDSO yields ultrathin, smooth, and homogenous films whose organic/inorganic character can be controlled through the reaction conditions.
- At low powers, the system is monomer-deficient, and the deposition rate is highly flow rate-dependent. At high powers, the system reaches an energy saturation, and the deposition rate is relatively flow rate-independent.
- PPHMDSO films contain atmospheric oxygen that has reacted with long-lived radicals in the polymer. At high flow rates and low powers, the similarity between the plasma polymer and the monomer is the greatest. At high powers, the monomer is severely fragmented, and the structure becomes more inorganic in nature.
- The plasma polymer structure seems to be a silicon-oxygen network with short hydrocarbon chains that may include hydroxyl and/or carbonyl groups attached to silicon in the backbone.
- The inorganic nature of the plasma polymer at high powers is reflected in its high polar surface tension.

The authors wish to gratefully acknowledge the support of the Water Research Institute, Technion–Israel Institute of Technology.

REFERENCES

1. H. Yasuda, *Plasma Polymerization,* Academic Press, London, 1985.
2. J. Sakata, M. Yamamoto, and M. Hirai, *J. Appl. Polym. Sci.,* **31,** 1999 (1986).
3. H. Matsuyama, A. Kariya, and M. Teramoto, *J. Appl. Polym. Sci.,* **51,** 689 (1994).

4. S. Cai, J. Fang, and X. Yu, *J. Appl. Polym. Sci.*, **44**, 135 (1992).
5. E. Radeva, D. Tsakov, K. Bobev, and L. Spassov, *J. Appl. Polym. Sci.*, **50**, 165 (1993).
6. F. Kokai, T. Kubota, M. Ichjyo, and K. Wakai, *J. Appl. Polym. Sci., Appl. Polm. Symp.*, **42**, 197 (1988).
7. M. Morra, E. Occhiello, and F. Garbassi, *J. Appl. Polym. Sci.*, **48**, 1331 (1993).
8. S. Y. Park and N. Kim, *J. Appl. Polym. Sci., Appl. Polym. Symp.*, **46**, 92 (1990).
9. F. Homilius, A. Heilmann, J. Werner, and W. Grunewald, *Phys. Stat. Sol (a)*, **137**, 145 (1993).
10. R. Rochotzki, M. Arzt, F. Blaschta, E. Kreybig, and H. U. Poll, *Thin Solids Films*, **234**, 463 (1993).
11. H. U. Poll, J. Meichsner, M. Arzt, M. Friedrich, R. Rochotzki, and E. Kreybig, *Surf. Coatings Technol.*, **59**, 365 (1993).
12. L. D. Cho and O. Ekengren, *J. Appl. Polym. Sci.*, **47**, 2125 (1993).
13. N. Inagaki, *Mol. Cryst. Liq. Cryst.*, **224**, 123 (1993).
14. J. Y. Lai, C. Y. Shih, and F. C. Lin, *Polymer J.*, **26**, 665 (1994).
15. P. M. Sherwood, in *Practical Surface Analysis by Auger and X-ray Photoelectron Spectroscopy*, D. Briggs and M. P. Seah, Eds., Wiley, New York, 1983, p. 465.
16. A. J. Kinloch, *Adhesion and Adhesives*, Chapman and Hall, New York, 1987.
17. D. K. Owens and R. C. Wendt, *J. Appl. Polym. Sci.*, **13**, 1741 (1969).
18. H. Yasuda, M. O. Bumgarner, H. C. March, and N. Morosoff, *J. Polym. Sci., Polym. Chem.*, **14**, 195 (1976).
19. A. M. Wrobel, *J. Macromol. Sci. Chem.*, **A22**, 1089 (1985).
20. P. Laoharojaphand, T. J. Lin, and J. O. Stoffer, *J. Polym. Sci.*, **40**, 369 (1990).
21. G. Beamson and D. Briggs, *High Resolution XPS of Organic Polymers*, Wiley, New York, 1992.
22. W. E. Morgan and R. V. Wazer, *J. Phys. Chem.*, **77**, 964 (1973).
23. R. C. Gray, J. C. Carver, and D. M. Hercules, *J. Elec. Spect. Relat. Phenom.*, **8**, 343 (1976).
24. N. B. Colthup, L. H. Daly, and S. E. Wiberley, *Introduction to Infrared and Raman Spectroscopy*, Academic Press, New York, 1964.
25. J. Brandrup and E. H. Immergut, *Polymer Handbook*, 3rd Ed., Wiley, New York, 1989.

Received June 21, 1995
Accepted March 19, 1996